



Published in final edited form as:

*Clin Cancer Res.* 2022 February 15; 28(4): 748–755. doi:10.1158/1078-0432.CCR-21-3088.

## Biomarkers of Angiogenesis and Clinical Outcomes to Cabozantinib and Everolimus in Patients with Metastatic Renal Cell Carcinoma from the Phase III METEOR Trial

Thomas Denize<sup>1,2</sup>, Subrina Farah<sup>3</sup>, Alessia Cimadamore<sup>1,2,4</sup>, Abdallah Faifel<sup>1,2</sup>, Emily Walton<sup>1</sup>, Maura A Sticco-Ivins<sup>1</sup>, Chris Labaki<sup>2,5</sup>, David A. Braun<sup>2,5,6</sup>, Maxine Sun<sup>5</sup>, Evelyn Wang<sup>7</sup>, Wanling Xie<sup>3</sup>, Toni K. Choueiri<sup>2,5,6</sup>, Sabina Signoretti<sup>1,2,6,8</sup>

<sup>1</sup>Department of Pathology, Brigham and Women's Hospital, Boston, MA 02115, USA

<sup>2</sup>Harvard Medical School, Boston, MA 02115, USA

<sup>3</sup>Department of Data Sciences, Dana-Farber Cancer Institute, Boston, MA 02115, USA

<sup>4</sup>Section of Pathological Anatomy, School of Medicine, Polytechnic University of the Marche Region, United Hospitals, Ancona 60126, Italy

<sup>5</sup>Department of Medical Oncology, Dana-Farber Cancer Institute, Boston, MA 02115, USA

<sup>6</sup>Broad Institute of MIT and Harvard, Cambridge, MA, USA

<sup>7</sup>Exelixis Inc., South San Francisco, CA, USA

<sup>8</sup>Department of Oncologic Pathology, Dana-Farber Cancer Institute, Boston, MA 02115, USA

### Abstract

**Purpose:** Anti-angiogenic VEGF-receptor (VEGFR) inhibitors are approved for metastatic clear cell renal cell carcinoma (mccRCC) and their efficacy is higher in high angiogenic tumors. As cabozantinib inhibits multiple tyrosine kinase receptors, including VEGFRs, we tested whether markers of angiogenesis, including microvascular density (MVD) and mast cell density (MCD), could predict benefit from cabozantinib versus everolimus, using RCC samples from the METEOR (NCT01865747) trial.

**Experimental design:** MVD and MCD were studied in 430 patients (cabozantinib = 216, everolimus = 214) by double immunohistochemistry for CD31 (vascular marker) and tryptase (mast cell marker) coupled with automated image analysis. Results from evaluable cases (MVD = 360, MCD = 325) were correlated with progression-free survival (PFS), overall survival (OS), and objective response rate (ORR).

**Results:** MVD was positively correlated with MCD. In the whole cohort, high MVD and high MCD were associated with longer PFS; improved PFS was most evident in patients with high levels of both MCD and MVD. Cabozantinib was associated with improved PFS, OS, and ORR compared to everolimus, irrespective of MVD levels. Cabozantinib was also associated

**Corresponding author:** Sabina Signoretti, M.D., Brigham and Women's Hospital, Thorn Building 504A, 75 Francis Street; Boston, MA 02115, +1 617-525-7437, ssignoretti@bwh.harvard.edu.

T.D. A.F. M.S.I Em. W. S.F. C.L. declare no conflicts of interest.

with improved ORR compared to everolimus, irrespective of MCD levels. For PFS and OS, the treatment effect for cabozantinib versus everolimus tended to be greater in tumors with low MCD.

**Conclusions:** High MVD and high MCD are associated with improved outcome in mcrRCC but don't predict efficacy to cabozantinib versus everolimus. The high efficacy of cabozantinib in low angiogenic tumors allows us to speculate that its anti-tumor activity is not exclusively mediated by VEGFR inhibition.

### Keywords

Renal Cell Carcinoma (RCC); Cabozantinib; Biomarker; Angiogenesis; Microvascular density; Mast cells

## Introduction

Vascular endothelial growth factor receptors (VEGFR)-tyrosine kinase inhibitors (TKIs) are approved treatments for patients with metastatic clear cell renal cell carcinoma (mcrRCC), either as monotherapy or in combination with anti-PD-1 agents. There is both preclinical and clinical evidence that in ccRCC, the anti-tumor activity of VEGFR-TKIs is largely mediated by their anti-angiogenic effect<sup>1-3</sup>. Of note, recent data indicate that ccRCC tumors with high levels of tumor vascularization respond better to these anti-angiogenic agents. Indeed, in mcrRCC patients treated with the VEGFR-TKI sunitinib as part of the IMmotion 150 and IMmotion 151 trials, high expression of a 6-gene angiogenesis signature, including *PECAMI* (coding for CD31) was associated with improved ORR and PFS<sup>4,5</sup>. As expected, the angiogenesis gene signature levels were strongly associated with levels of microvascular density (MVD), assessed by CD31 immunohistochemistry, which is a well-established biomarker of angiogenesis<sup>4</sup>. More recently, results from IMmotion 150/151 trials were independently confirmed by analysis of the JAVELIN Renal 101 trial<sup>6</sup>.

Cabozantinib is a multitarget TKI active against VEGFR, Met, and Axl, among others. The METEOR (NCT01865747) trial demonstrated cabozantinib to be an effective drug in treating mcrRCC patients who progressed after previous VEGFR-TKI treatment<sup>7</sup>. In addition, cabozantinib has been shown to be more effective than sunitinib in the first-line setting<sup>8</sup>. More recently, the combination of cabozantinib plus the anti-PD-1 antibody nivolumab was also shown to be superior to sunitinib for the frontline treatment of patients with mcrRCC<sup>9</sup>.

Currently, it remains unclear whether cabozantinib superiority over earlier VEGFR-TKIs (i.e., sunitinib) is due to the inhibition of additional tyrosine kinase receptors (RTKs) (e.g., Met and Axl) or to more potent inhibition of VEGFR<sup>10,11</sup>. Understanding whether, similar to sunitinib, cabozantinib is more effective in patients with high-angiogenic tumors would not only provide insights into the role of VEGFR-inhibition in mediating the anti-tumor activity of cabozantinib in mcrRCC, but could also lead to the identification of biomarkers of response to this agent, alone or in combination with other drugs. For these reasons, we tested the prognostic and predictive value of makers of angiogenesis in pretreatment tumor tissues from patients who received either cabozantinib or everolimus within the METEOR trial. We decided to focus on protein markers analyzed by immunohistochemistry

(IHC) because, in contrast to RNA-based biomarkers, they are very cost-effective and can be widely implemented in diagnostic laboratories throughout the world. Specifically, we measured MVD by assessing CD31 expression on endothelial cells in whole tissue sections. Moreover, we quantified intratumoral mast cell infiltration (using IHC for tryptase) as these immune cells are known to promote angiogenesis in various cancer types, both through VEGF-dependent and -independent pathways<sup>12–20</sup>. Of note, in RCC, mast cells have been shown to stimulate angiogenesis both *in vitro* and *in vivo*, and mast cell infiltration has been associated with angiogenesis in patient samples<sup>12,21</sup>.

## Materials and Methods

### Study Design and Clinical Endpoints

Microvascular density (MVD) and Mast Cell density (MCD) were assessed on pretreatment tumor tissue samples (archival nephrectomy specimens n= 399 or metastases biopsy n= 31) of patients from the METEOR randomized phase III clinical trial. In the METEOR trial, cabozantinib was compared to everolimus in patients with mRCC who had progressed after previous VEGF TKI treatment<sup>22</sup>. Baseline demographics, clinical characteristics, and treatment outcomes, including objective response rate (ORR, including complete response and partial response), progression-free survival (PFS), and overall survival (OS), were collected from the trial database. PFS and ORR (per RECIST 1.1) were determined by an independent radiology review committee assessment. PFS was defined as the time from randomization to radiographic progression or death from any cause and censored at the date of last disease assessment; OS was calculated from randomization to date of death from any cause and censored at the date of last follow up.

This study was approved by the Institutional Review Board or ethics committee of the participating centers and was conducted in accordance with the Declaration of Helsinki and the Good Clinical Practice guidelines. All patients provided written informed consent.

### Immunohistochemistry Staining

IHC staining was performed on formalin-fixed paraffin-embedded (FFPE) tissue sections collected by the study sponsors at enrollment. An in-house double IHC staining assay was developed using an anti-CD31 antibody (1:100, JC70A mouse monoclonal antibody, Agilent Cat# GA610, RRID:AB\_2892053) and an anti-tryptase antibody (1:5000, AA1 mouse monoclonal antibody, Agilent Cat# M7052, RRID:AB\_2206478). Performance of antibodies against CD31 and tryptase was validated on non-neoplastic kidney tissue to obtain a staining pattern in accordance with available published data.

Tumor sections were stained with a Bond III Autostainer (Leica Biosystems) using a Bond Polymer Refine Detection Kit (DS9800; Leica Biosystems) for the anti-CD31 stain and a Bond Polymer Refine Red Detection Kit (DS9390, Leica Biosystems) for the anti-tryptase stain. Antigen retrieval was performed with Bond Epitope Retrieval Solution 2 (EDTA, pH = 9.0) for 20 minutes before the anti-CD31 stain. Following the anti-CD31 staining, antibody stripping was performed with Bond Epitope Retrieval Solution 1 (Citrate, pH = 6.0) for 10

minutes prior to the anti-tryptase stain. All slides were counterstained with hematoxylin, dehydrated in graded ethanol and xylene, mounted, and coverslipped.

Met and PD-L1 protein expression data were available from previous studies<sup>7,23</sup>.

### **Image Analysis for assessment of MVD and MCD**

Immunostained slides were scanned at 20x magnification using an Aperio Versa (Leica Biosystems) and analyzed using Indica Lab HALO platform algorithms. For each slide, tumor areas were manually annotated by research assistants (EW, MSI) and reviewed by pathologists (TD, AC). Areas of necrosis and intervening stroma were excluded from the analysis. Background staining, as well as macrophages positive for CD31 expression, were excluded using the HALO platform tissue classification module. The number of microvessels and mast cells was determined using the HALO platform colocalization v1.3 algorithm. Seventy patient samples were excluded on the MVD analysis due to absence of tumor or technical reasons; of the 360 samples analyzed for MVD, 35 were excluded of the MCD analysis due to technical reasons (Supplementary Figure 1). For each immunostained slide, two pathologists (TD, AC) confirmed that i) the algorithms correctly identified the microvessels and the mast cells, and ii) the classifier correctly excluded the macrophages stained by the anti-CD31 antibody. MVD and MCD were then calculated for each slide. For patients with multiple tissue samples, the highest MVD and associated MCD were used for subsequent analyses. All pathologists were blinded to the patient clinical outcomes.

### **Statistical analysis**

To explore the association of MVD and MCD with clinical outcomes, initially patients were grouped into low, medium and high levels based on using the tertile cut-points for each measure. Since low and medium tertile levels featured similar association with outcomes, therefore two groups were merged, and each measure was dichotomized at the upper 33 percentile value for the 'high' group.

To evaluate the association of MVD and MCD by IMDC risk group, tumor grade, MET and PD-L1 status Wilcoxon rank sum test was applied. To check association between MVD/MCD and MET and PD-L1 status generalized linear models were considered adjusted for tumor grades.

Distributions of PFS and OS were estimated using Kaplan Meier methodology along with a 95% confidence interval (95%CI). Both univariate and multivariable Cox proportional hazards models were conducted to estimate association with PFS and OS; Wald chi square test was provided. The multivariable models were adjusted for treatment, IMDC risk group, presence of bone metastases and number of previous VEGFR TKI treatment (1 or 2). Cochran-Armitage trend test was used to compare ORR among the ordered levels. Fisher's exact test was conducted to compare ORR for dichotomized markers.

To explore the predictive value of the MCD and MVD, we fit Cox regression models with the interaction term of treatment group and each biomarker and assessed hazard ratio for treatment comparison on PFS and OS by MCD and MVD levels (high and low), both unadjusted and adjusted interaction models were calculated. Test for interaction (p-

interaction) was provided to assess whether treatment effects differed by biomarker groups. Unadjusted logistic regression model was conducted to assess treatment effects differed by biomarker groups for ORR.

Similar analyses were conducted for the combination of MCD and MVD and the combination of two biomarkers with Met status.

SAS version v9.4 (Cary, NC, USA) was used to carry out the above analysis. All statistical tests were two-sided.

### **Data availability statement**

The data generated in this study are available upon request from the corresponding author.

## **Results**

### **Patients characteristics and treatment**

From August 2013 to November 2014, 658 patients were enrolled in the METEOR trial and randomly assigned (1:1) to receive either cabozantinib (n=330) or everolimus (n=328) as previously described<sup>7</sup>. Data cut-off was May 22, 2015 for PFS and response evaluation, while for OS the data cutoff was December 31, 2015.

MVD and MCD density were studied in 430 patients (cabozantinib = 216, everolimus = 214) with tissue available tissue specimens. Evaluable data were obtained in 360 patients (cabozantinib = 175, everolimus = 185) for MVD. Among these 360 patients, 325 patients (cabozantinib = 159, everolimus = 166) had evaluable data for MCD (Supplementary Figure 2). Patient demographic and clinical characteristics were similar in the subset of patients with available tissue specimens as compared with the overall trial population (Supplementary Table 1).

### **Association of microvascular density and mast cell density with clinicopathological features**

Median MVD and MCD were 147 MV/mm<sup>2</sup> (range 8.8–750.4) and 7 MC/mm<sup>2</sup> (range 0–72.8 MC/mm<sup>2</sup>), respectively. In line with previous studies, we observed that MVD was positively correlated to MCD, with a Spearman correlation coefficient of 0.42 (p<0.0001) (Supplementary Figure 3).

Both MVD and MCD were found to be negatively associated with tumor grade (p< 0.0001 for MVD and p=0.04 for MCD). Moreover, MCD levels were associated with IMDC risk groups at baseline, with higher levels observed in patients with favorable risk (p=0.006). Finally, MVD levels were higher in tumors negative for PD-L1 expression and in tumors negative for Met expression (Supplementary Table 2).

### **Association of microvascular density with clinical outcomes**

As previous studies have shown that MVD is associated with favorable prognosis in localized ccRCC<sup>24</sup>, we investigated its association with clinical outcome in patients with mcrRCC treated with targeted therapies. In the initial analysis, the low and medium

tertile groups featured similar associations with outcomes (Supplementary Figure 4a–b) and, therefore, the upper tertile cut-point was selected to categorize patients in MVD-high and MVD-low dichotomous groups. In the whole cohort, patients with high MVD had significantly longer median PFS compared with patients with low MVD (7.3 months vs. 5.4 months, HR 0.66, 95% CI 0.50–0.88), on univariate analysis (Table 1, Figure 1a). In multivariable model, adjusted for treatment, IMDC risk group, presence of bone metastases, and number of previous VEGFR TKI treatment (1 or 2), the significant differences in PFS remained (adjusted HR 0.69, 95% CI 0.52–0.93) (Table 1). MVD was not associated with ORR (Supplementary Table 3) or OS (Table 1, Figure 1b).

Since the mechanism of action of cabozantinib involves inhibition of angiogenesis by targeting tyrosine kinase receptors, including VEGFRs, we hypothesized that patients with high MVD would receive greater benefit from cabozantinib compared to patients with low MVD. In contrast to our expectation, treatment with cabozantinib was associated with improved PFS, OS, and ORR compared to everolimus, irrespective of MVD levels in both univariate and multivariable models (Table 2, Figure 2a–b, Supplementary Figure 5a–b, Supplementary Table 4). Moreover, analysis of clinical outcome by MVD status in each treatment arm revealed that while everolimus-treated patients with high MVD had longer median PFS compared to patients with low MVD (7.3 months vs 3.8 months; adjusted HR 0.63; 95% CI 0.42–0.95), the association between PFS and MVD status was less evident in the cabozantinib arm (9.0 vs 7.3 months, adjusted HR 0.77; 95% CI 0.50–1.18, Table 2). MVD was not associated with ORR (Supplementary Table 4) or OS (Table 2) in either the cabozantinib or the everolimus arm.

### Association of mast cell density with clinical outcomes

Intratumoral MC infiltration has been associated with angiogenesis in the context of ccRCC, but its prognostic and predictive value remains unknown. Therefore, we first tested for an association between MCD and clinical outcome in our patient cohort. The low and medium tertile groups displayed similar associations with outcomes (Supplementary Figure 4c–d); therefore, the upper tertile cut-point was selected to categorize patients in MCD-high and MCD-low dichotomous groups. On univariate analysis, both median PFS and OS were significantly longer in patients with high MCD compared with patients with low MCD (PFS: 7.5 vs 5.5 months, HR 0.64; 95% CI 0.47–0.87; OS: NR vs 18.4 months, HR 0.66; 95% CI 0.44–0.92) (Table 1, Figure 1c–d). Similar results were observed in multivariable models for both PFS (adjusted HR 0.66; 95% CI 0.48–0.91) and OS (adjusted HR 0.69; 95% CI 0.48–0.99) (Table 1). There was no association between MCD and ORR (Supplementary Table 3).

We then assessed the predictive value of MCD by comparing outcomes on cabozantinib versus everolimus in patients with high and low MCD. Treatment with cabozantinib was associated with improved ORR compared to everolimus, irrespective of MCD levels in both univariate and multivariable models (Supplementary Table 4). For PFS and OS, however, the magnitude of treatment effect for cabozantinib versus everolimus was numerically larger in MCD-low group compared to MCD-high group, though the interaction test did not meet the conventional level of significance ( $p$ -interaction=0.11 for PFS and  $p$ -interaction=0.24 for

OS) (Table 2, Figure 2c–d, Supplementary Figure 5c–d). When we tested for an association between MCD and clinical outcome within each treatment arm, we found that in the everolimus arm, patients with high MCD had significantly longer median PFS and OS than patients with low MCD (PFS: 7.5 months vs 3.8 months; adjusted HR 0.51; 95% CI 0.32–0.79 and OS: NR vs 15.4 months; adjusted HR 0.56; 95% CI 0.34–0.94). In contrast, no association between MCD and PFS or OS was detected in the cabozantinib arm (adjusted HR 0.85, 95% CI: 0.54–1.34 for PFS and 0.88, 95% CI: 0.51–1.52 for OS, Table 2). MCD was not associated with ORR in either the cabozantinib or the everolimus arm (Supplementary Table 4).

### **Association of combined microvascular density and mast cell density with clinical outcomes**

We further investigated the prognostic and predictive role of the two markers by stratifying patients in three groups according to dichotomous MVD levels combined with dichotomous MCD levels. Patients with high levels of either MCD or MVD (high/low or low/high) had significantly longer PFS compared to patients with low levels of both markers (MVD-low/MCD-low) (6.5 months vs 4.7 months; adjusted HR 0.69, 95% CI 0.49–0.97). Improved PFS was most evident in patients with high levels in both MCD and MVD (MVD-high/MCD-high) versus MVD-low/MCD-low patients (9.1 months vs 4.7 months; adjusted HR 0.57, 95% CI 0.38–0.85) (Figure 1e, Supplementary Table 5). No difference in ORR or OS was observed among the three patient groups identified by combined MVD/MCD levels (Figure 1f, Supplementary Tables 5 and 6).

When the predictive value of the combined markers was assessed, treatment with cabozantinib was found to be associated with improved OS and ORR compared to everolimus, irrespective of the combined MVD/MCD levels. For PFS, the magnitude of treatment effect for cabozantinib versus everolimus was numerically larger in MVD-low/MCD-low group, though the interaction test was not significant ( $p$ -interaction=0.26) (Supplementary Tables 7 and 8). Analysis of clinical outcome by combined MVD/MCD status in each treatment arm showed that in the everolimus arm, both PFS and OS were significantly longer in MVD-high/MCD-high patients compared to MVD-low/MCD-low patients (PFS: 9.1 months vs 3.7 months; adjusted HR 0.45, 95% CI 0.26–0.76 and OS: 20.4 months vs 15.9 months; adjusted HR 0.61, 95% CI 0.34–1.13); only PFS was significantly longer in patients with high levels of either MCD or MVD (high/low or low/high) compared to MVD-low/MCD-low patients (PFS: 5.5 months vs 3.7 months; adjusted HR 0.58, 95% CI 0.35–0.96). Conversely, no association between combined MVD/MCD levels and PFS or OS was observed in the cabozantinib arm. No difference in ORR was observed among the three patient groups identified by combined MVD/MCD levels in either the cabozantinib or the everolimus arm (Supplementary Tables 7 and 8).

### **Association of Met expression combined with microvascular density or mast cell density with clinical outcomes.**

As Met is one of the targets of cabozantinib, we explored the impact of its expression (previously assessed by IHC)<sup>23</sup> combined with MVD or MCD on clinical outcomes.

To analyze the combined expression of Met and MVD, we considered two main groups (due to the small number of patients in some subgroups): 1) patients without expression of Met and low MVD (MVD-low/Met-negative), 2) patients with either Met expression, or high MVD, or both (MVD-high and/or Met-positive). Improved PFS on cabozantinib relative to everolimus was observed in both MVD-low/Met-negative and MVD-high and/or Met-positive patients. Similar results were observed for ORR (Supplementary Tables 9 and 10). For OS, the magnitude of treatment effect for cabozantinib versus everolimus was numerically greater for MVD-high and/or Met-positive patients compared to MVD-low/Met-negative patients, though the interaction test was not significant (p-interaction=0.20) (Supplementary Table 9).

Similar to MVD/Met analysis, evaluation of combined MCD/Met data was conducted by grouping patients with low MCD and negative Met expression, and comparing them to patients with either high MCD, or positive Met expression, or both. Treatment with cabozantinib was found to be associated with improved PFS, OS, and ORR compared to everolimus both in MCDlow/ Met-negative patients and in MCDhigh and/or Met-positive patients (Supplementary Tables 9 and 10).

## Discussion

Our analyses of tumor tissue samples from the METEOR trial showed that high levels of tumor angiogenesis markers (i.e., MVD and MCD) are not predictive of efficacy to cabozantinib relative to everolimus but are associated with longer PFS in the entire patient cohort. However, when the treatment arms were analyzed separately, this association remained among patients treated with everolimus but was less evident among patients treated with cabozantinib. Moreover, the PFS improvement with cabozantinib versus everolimus was numerically greater in patients with low levels of tumor angiogenesis markers. These results are somewhat at odds with recent results from several clinical trial cohorts consistently showing that in sunitinib-treated patients, high levels of tumor angiogenesis (measured by an angiogenesis signature) are associated with better clinical outcome<sup>4-6</sup>.

Sunitinib is a potent inhibitor of VEGFR, platelet-derived growth factor receptor (PDGFR), and c-Kit, and preclinical data demonstrated that it exerts both anti-angiogenesis and anti-tumor effects<sup>25</sup>. In xenograft models of ccRCC, sunitinib was shown to dramatically reduce tumor vascularization and induce tumor cell necrosis<sup>26,27</sup>. In patients with mcrRCC treated VEGFR TKIs (including sunitinib), an on-treatment decrease in arterial spin-labeled (ASL) MRI perfusion was associated with tumor response<sup>2</sup>. Overall, these data suggest that in mcrRCC, sunitinib acts primarily through an anti-angiogenic mechanism. The recent findings that sunitinib is more effective in mcrRCC patients with a high angiogenic gene signature is in line with this hypothesis.

On the other hand, the mechanism of action of cabozantinib in kidney cancer has been unclear. Compared to sunitinib, cabozantinib is a more potent VEGFR2 inhibitor<sup>10,11</sup>, raising the possibility that its higher efficacy in ccRCC is largely due to a stronger inhibition of tumor vascularity. However, cabozantinib inhibits additional RTKs, including



Met and Axl, which are known to play an important role in ccRCC biology and have been implicated in cell growth invasion, invasion metastasis, angiogenesis, and resistance to sunitinib therapy<sup>10,28–30</sup>. Our findings show that, contrary to sunitinib, cabozantinib is highly effective in mcrRCC patients with low levels of tumor angiogenesis. On the basis of these results, we speculate that cabozantinib mechanism of action might not exclusively rely on its potent VEGFR2 inhibition but could involve tumor intrinsic inhibition of Met, Axl, and potentially other RTKs. Our finding that OS improvement with cabozantinib versus everolimus tends to be greater for patients with high MVD and/or Met-positive tumors compared to patients with both low MVD and Met-negative tumors seems to support this possibility. Given that cabozantinib displays a high spectrum of activity against multiple signaling pathways, the identification of predictors of response likely requires the development of a combined multi-marker model; such model might need to integrate genomic-, transcriptomic-, and protein-based biomarkers. As preclinical studies have also suggested a possible immunomodulatory function of cabozantinib in RCC<sup>31</sup>, future investigations should also include an in-depth characterization of the tumor microenvironment.

In this work, we confirmed the presence of a strong correlation between MVD and MCD in ccRCC, as previously reported<sup>12,21</sup>. Moreover, we demonstrated that both MVD and MCD are negatively associated with tumor grade. These findings are consistent with previously published results from the ECOG-ACRIN 2805 trial demonstrating that in localized high-risk RCC, high levels of angiogenesis (measured by MVD) are associated with favorable histopathologic features and improved OS<sup>24</sup>. Similar to MVD, high MCD was also previously reported as favorable prognostic factor in non-metastatic ccRCC<sup>32</sup>. Along these lines, we found that in patients treated with everolimus, both high MVD and high MCD were associated with longer PFS, and high MCD was also associated with longer OS. It is uncertain, however, whether these results simply reflect the indolent clinical behavior of high-angiogenic tumors or might be also linked to a possible anti-angiogenic effect of MTOR inhibition.

Although MVD and high MCD were found to be highly correlated, the combination of the two biomarkers further stratified patient outcomes in the whole patient cohort and in the everolimus arm. Indeed, improved PFS was most evident in patients with high levels of both MCD and MVD. These data indicate that the role of MVD and MCD as biomarkers is not completely overlapping and suggest that tumor-infiltrating mast cells may play a role in the tumor microenvironment that goes beyond the induction of angiogenesis<sup>33</sup>.

This study presents several limitations. First, our analyses were performed in archival tissues that were mostly collected before the patients received any systemic therapy. Therefore, these samples are not representative of the changes in tumor biology that might have been induced by treatments received prior to cabozantinib. Second, the tissue slides used for immunohistochemistry were obtained from institutions worldwide, which likely have different tissue handling, fixation, and processing protocols that differently affect the immunoreactivity of the samples. This is a general issue related to the analysis of clinical trial specimens that in our study was at least in part overcome by the fact that assessment of MVD and MCD did not require quantification of staining intensity, and

thus less immunoreactive slides could be reliably analyzed as long as specific staining was present. Finally, our studies were conducted on a single tumor section per patient. While this approach does not fully address possible intratumoral heterogeneity, in order to mitigate this issue, we developed image analysis protocols that allowed us to obtain data from the whole tissue section rather than focusing on small selected regions of interest, as frequently done in tissue-based biomarker investigations.

## Supplementary Material

Refer to Web version on PubMed Central for supplementary material.

## Acknowledgments of research support for the study:

This work was supported by R21 CA238053-01, Dana-Farber / Harvard Cancer Center Kidney Cancer SPORE (P50-CA101942-12), and Exelixis Inc. T.K.C. is supported in part by the Program 5P30CA006516-56, the Kohlberg Chair at Harvard Medical School and the Trust Family, Michael Brigham, and Loker Pinard Funds for Kidney Cancer Research at DFCI.

Conflicts of interests:

T.K.C reports Research/advisory boards/consultancy/Honorarium (Institutional and personal): AstraZeneca, Aravive, Aveo, Bayer, Bristol Myers-Squibb, Eisai, EMD Serono, Exelixis, GlaxoSmithKline, IQVA, Ipsen, Lilly, Merck, Novartis, Pfizer, Roche, Sanofi/Aventis, Takeda, Tempest, Up-To-Date, CME events (Peerview, OncLive and others)

D.A.B. reports nonfinancial support from Bristol Myers Squibb, honoraria from LM Education/Exchange Services, and personal fees from Octane Global, Defined Health, Dedham Group, Adept Field Solutions, Slingshot Insights, Blueprint Partnerships, Charles River Associates, Trinity Group, Insight Strategy, Exelixis, and MDedge, outside of the submitted work.

Ev.W. is a shareholder of Exelixis stock.

A.C. reports personal fees from AstraZeneca outside of the submitted work.

W.X. reports Consultant to “Convergent Therapeutics, Inc”.

S.S. reports receiving commercial research grants from Bristol-Myers Squibb, AstraZeneca, Exelixis and Novartis; is a consultant/advisory board member for Merck, AstraZeneca, Bristol-Myers Squibb, CRISPR Therapeutics AG, AACR, and NCI; and receives royalties from Biogenex.

## References

1. Wilhelm SM, Carter C, Tang LY, Wilkie D, McNabola A, Rong H, et al. BAY 43–9006 exhibits broad spectrum oral antitumor activity and targets the RAF/MEK/ERK pathway and receptor tyrosine kinases involved in tumor progression and angiogenesis. *Cancer Res.* 2004;64(19):7099–7109. [PubMed: 15466206]
2. Tsai LL, Bhatt RS, Strob MF, Jegede OA, Sun MRM, Alsop DC, et al. Arterial Spin Labeled Perfusion MRI for the Evaluation of Response to Tyrosine Kinase Inhibition Therapy in Metastatic Renal Cell Carcinoma. *Radiology.* 2021;298(2):332–340. [PubMed: 33258745]
3. Le Tourneau C, Raymond E, Faivre S. Sunitinib: A novel tyrosine kinase inhibitor. A brief review of its therapeutic potential in the treatment of renal carcinoma and gastrointestinal stromal tumors (GIST). *Ther Clin Risk Manag.* 2007;3(2):341–348. [PubMed: 18360643]
4. McDermott DF, Huseni MA, Atkins MB, Motzer RJ, Rini BI, Escudier B, et al. Clinical activity and molecular correlates of response to atezolizumab alone or in combination with bevacizumab versus sunitinib in renal cell carcinoma. *Nat Med.* 2018;24(6):749–757. [PubMed: 29867230]

5. Motzer RJ, Banchereau R, Hamidi H, Powles T, McDermott D, Atkins MB, et al. Molecular Subsets in Renal Cancer Determine Outcome to Checkpoint and Angiogenesis Blockade. *Cancer Cell*. November 2020:1–15.
6. Motzer RJ, Robbins PB, Powles T, Albiges L, Haanen JB, Larkin J, et al. Avelumab plus axitinib versus sunitinib in advanced renal cell carcinoma: biomarker analysis of the phase 3 JAVELIN Renal 101 trial. *Nat Med*. 2020;26(11):1733–1741. [PubMed: 32895571]
7. Choueiri TK, Escudier B, Powles T, Tannir NM, Mainwaring PN, Rini BI, et al. Cabozantinib versus everolimus in advanced renal cell carcinoma (METEOR): final results from a randomised, open-label, phase 3 trial. *Lancet Oncol*. 2016;17(7):917–927. [PubMed: 27279544]
8. Choueiri TK, Halabi S, Sanford BL, Hahn O, Michaelson MD, Walsh MK, et al. Cabozantinib versus sunitinib as initial targeted therapy for patients with metastatic renal cell carcinoma of poor or intermediate risk: The alliance A031203 CABOSUN trial. *J Clin Oncol*. 2017;35(6):591–597. [PubMed: 28199818]
9. Choueiri TK, Powles T, Burotto M, Escudier B, Bourlon MT, Zurawski B, et al. Nivolumab plus Cabozantinib versus Sunitinib for Advanced Renal-Cell Carcinoma. *N Engl J Med*. 2021;384(9):829–841. [PubMed: 33657295]
10. Yakes FM, Chen J, Tan J, Yamaguchi K, Shi Y, Yu P, et al. Cabozantinib (XL184), a novel MET and VEGFR2 inhibitor, simultaneously suppresses metastasis, angiogenesis, and tumor growth. *Mol Cancer Ther*. 2011;10(12):2298–2308. [PubMed: 21926191]
11. Choueiri TK, Kaelin WG. Targeting the HIF2–VEGF axis in renal cell carcinoma. *Nat Med*. 2020;26(10):1519–1530. [PubMed: 33020645]
12. Chen Y, Li C, Xie H, Fan Y, Yang Z, Ma J, et al. Infiltrating mast cells promote renal cell carcinoma angiogenesis by modulating PI3K → AKT → GSK3β → AM signaling. *Oncogene*. 2017;36(20):2879–2888. [PubMed: 28114284]
13. De Palma M, Biziato D, Petrova TV. Microenvironmental regulation of tumour angiogenesis. *Nat Rev Cancer*. 2017;17(8):457–474. [PubMed: 28706266]
14. Guo X, Zhai L, Xue R, Shi J, Zeng Q, Gao C. Mast cell tryptase contributes to pancreatic cancer growth through promoting angiogenesis via activation of angiopoietin-1. *Int J Mol Sci*. 2016;17(6).
15. Visciano C, Prevece N, Liotti F, Marone G. Tumor-Associated Mast Cells in Thyroid Cancer. *Int J Endocrinol*. 2015;2015.
16. Ammendola M, Sacco R, Vescio G, Zuccalà V, Luposella M, Patruno R, et al. Tryptase mast cell density, protease-activated receptor-2 microvascular density, and classical microvascular density evaluation in gastric cancer patients undergoing surgery: possible translational relevance. *Therap Adv Gastroenterol*. 2017;10(4):353–360.
17. Feoktistov I, Ryzhov S, Goldstein AE, Biaggioni I. Mast Cell–Mediated Stimulation of Angiogenesis. *Circ Res*. 2003;92(5):485–492. [PubMed: 12600879]
18. Ribatti D, Crivellato E. Mast cells, angiogenesis, and tumour growth. *Biochim Biophys Acta - Mol Basis Dis*. 2012;1822(1):2–8.
19. Hiromatsu Y, Toda S. Mast cells and angiogenesis. *Microsc Res Tech*. 2003;60(1):64–69. [PubMed: 12500262]
20. Saxena S, Singh A, Singh P. Tumor associated mast cells: biological roles and therapeutic applications. *Anat Cell Biol*. 2020;53(3):245–251. [PubMed: 32879056]
21. Tuna B, Yorukoglu K, Unlu M, Mungan MU, Kirkali Z. Association of Mast Cells with Microvessel Density in Renal Cell Carcinomas. *Eur Urol*. 2006;50(3):530–534. [PubMed: 16426730]
22. Choueiri TK, Escudier B, Powles T, Mainwaring PN, Rini BI, Donskov F, et al. Cabozantinib versus Everolimus in Advanced Renal-Cell Carcinoma. *N Engl J Med*. 2015;373(19):1814–1823. [PubMed: 26406150]
23. Flaifel A, Xie W, Braun DA, Ficial M, Bakouny Z, Nassar AH, et al. PD-L1 Expression and Clinical Outcomes to Cabozantinib, Everolimus, and Sunitinib in Patients with Metastatic Renal Cell Carcinoma: Analysis of the Randomized Clinical Trials METEOR and CABOSUN. *Clin Cancer Res*. 2019;25(20):6080–6089. [PubMed: 31371341]

24. Jilaveanu LB, Puligandla M, Weiss SA, Wang XV, Zito C, Flaherty KT, et al. Tumor microvessel density as a prognostic marker in high-risk renal cell carcinoma patients treated on ECOG-ACRIN E2805. *Clin Cancer Res.* 2018;24(1):217–223. [PubMed: 29066509]
25. Carrato Mena A, Grande Pulido E, Guillén-Ponce C. Understanding the molecular-based mechanism of action of the tyrosine kinase inhibitor: Sunitinib. *Anticancer Drugs.* 2010;21(SUPPL.1):3–11.
26. Voce P, D'Agostino M, Moretti S, Sponziello M, Rhoden K, Calcinaro F, et al. Sunitinib inhibits tumor vascularity and growth but does not affect Akt and ERK phosphorylation in xenograft tumors. *Oncol Rep.* 2011;26(5):1075–1080. [PubMed: 21850379]
27. Bhatt RS, Wang X, Zhang L, Collins MP, Signoretti S, Alsop DC, et al. Renal cancer resistance to antiangiogenic therapy is delayed by restoration of angiostatic signaling. *Mol Cancer Ther.* 2010;9(10):2793–2802. [PubMed: 20699227]
28. Comoglio PM, Trusolino L, Boccaccio C. Known and novel roles of the MET oncogene in cancer: A coherent approach to targeted therapy. *Nat Rev Cancer.* 2018;18(6):341–358. [PubMed: 29674709]
29. Gay CM, Balaji K, Byers LA. Giving AXL the axe: Targeting AXL in human malignancy. *Br J Cancer.* 2017;116(4):415–423. [PubMed: 28072762]
30. Zhou L, Liu XD, Sun M, Zhang X, German P, Bai S, et al. Targeting MET and AXL overcomes resistance to sunitinib therapy in renal cell carcinoma. *Oncogene.* 2016;35(21):2687–2697. [PubMed: 26364599]
31. Liu H, Sun S, Wang G, Lu M, Zhang X, Wei X, et al. Tyrosine Kinase Inhibitor Cabozantinib Inhibits Murine Renal Cancer by Activating Innate and Adaptive Immunity. *Front Oncol.* 2021;11(April):1–15.
32. Fu H, Zhu Y, Wang Y, Liu Z, Zhang J, Wang Z, et al. Tumor Infiltrating Mast Cells (TIMs) Confers a Marked Survival Advantage in Nonmetastatic Clear-Cell Renal Cell Carcinoma. *Ann Surg Oncol.* 2017;24(5):1435–1442. [PubMed: 27896514]
33. Komi DEA, Redegeld FA. Role of Mast Cells in Shaping the Tumor Microenvironment. *Clin Rev Allergy Immunol.* 2020;58(3):313–325. [PubMed: 31256327]

**Statement of translational relevance**

Cabozantinib inhibits multiple tyrosine kinase receptors (RTKs), including VEGFRs, Met, and Axl, and is superior to VEGFR-inhibitors (i.e., sunitinib) in the treatment of metastatic clear cell renal cell carcinoma (mccRCC). However, it has been unclear whether its efficacy in kidney cancer is mainly due to anti-angiogenic effects mediated by its potent inhibition of VEGFRs or also involves tumor intrinsic targeting of additional RTKs. Using archival tumor samples from the METEOR trial, we demonstrated that, compared to everolimus, cabozantinib displays high efficacy in mccRCC regardless of the levels of tumor angiogenesis. Our findings suggest that cabozantinib might not simply work as an anti-angiogenic drug and that its mechanism of action involves the inhibition of multiple signaling pathways. This knowledge is critical for the future development of biomarkers of response to cabozantinib in mccRCC.

Author Manuscript

Author Manuscript

Author Manuscript

Author Manuscript

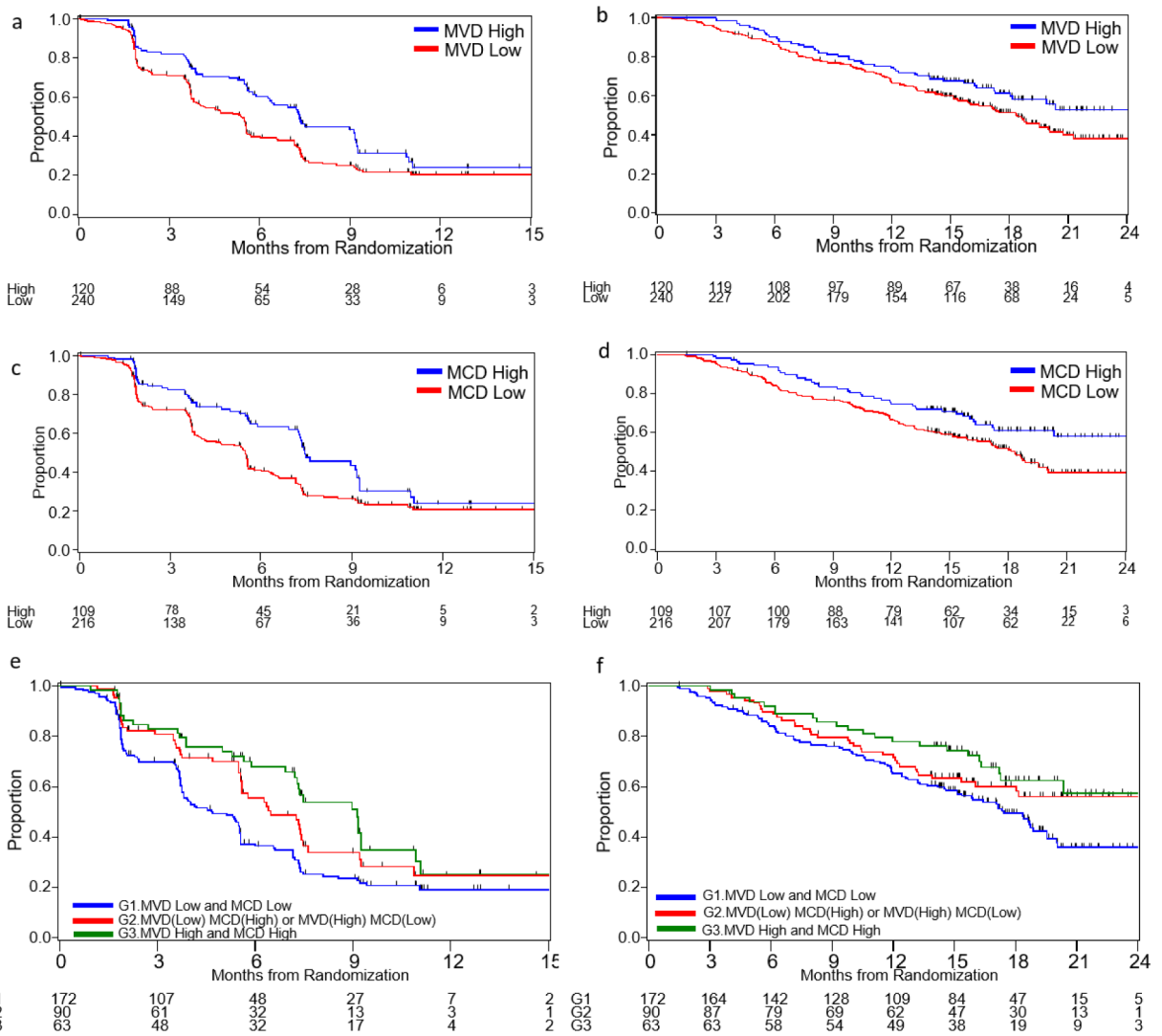


**Figure 1.** Kaplan-Meier curves of PFS and OS according to MVD, MCD, or combined MVD/MCD levels. a) PFS by MVD levels; b) OS by MVD levels; c) PFS by MCD levels d) OS by MCD levels; e) PFS by combined MVD/MCD levels; f) OS by combined MVD/MCD levels.

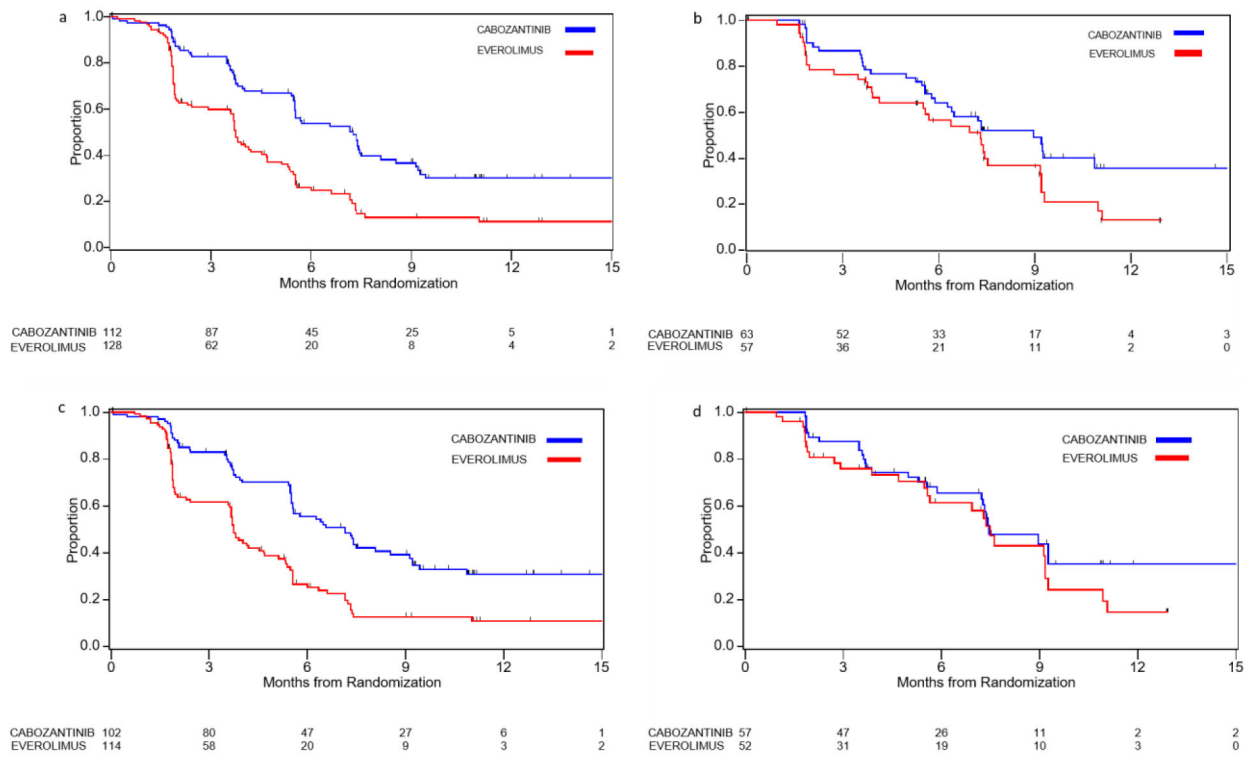


**Figure 2.** Kaplan Meier curves of PFS according to treatment in a) MVD Low group, b) MVD High group, c) MCD Low group, d) MCD high group.

**Table 1.**

Association of MVD and MCD dichotomous groups with PFS and OS.

	N. of events/ N. of Patients	Univariate Analysis		Multivariable Analysis	
		Months, Median (95% CI)	Unadjusted* HR (95% CI)	Adjusted* HR (95% CI)	Adjusted* p-value
<b>Microvascular density</b>					
<b>OS</b>					
Low ( < 208.2 mm <sup>2</sup> )	121/240	18.4 (15.9–20.0)	Ref.	Ref.	<i>0.1407</i>
High (>208.2 mm <sup>2</sup> )	48/120	NR (18.0-NR)	0.72 (0.51–1.00)	0.78 (0.55–1.09)	
<b>PFS</b>					
Low ( < 208.2 mm <sup>2</sup> )	154/240	5.4 (3.9–5.6)	Ref.	Ref.	<i>0.0144</i>
High (>208.2 mm <sup>2</sup> )	66/120	7.3 (6.3–9.2)	0.66 (0.50–0.88)	0.69 (0.52–0.93)	
<b>Mast cell density</b>					
<b>OS</b>					
Low ( < 11.3 mm <sup>2</sup> )	110/216	18.4 (15.9–19.6)	<i>Ref.</i>	<i>Ref.</i>	
High (>11.3 mm <sup>2</sup> )	39/109	NR (20.4-NR)	0.66 (0.44–0.92)	0.69 (0.48–0.99)	<i>0.0451</i>
<b>PFS</b>					
Low ( < 11.3 mm <sup>2</sup> )	142/216	5.5 (4.0–5.6)	<i>Ref.</i>	<i>Ref.</i>	
High (>11.3 mm <sup>2</sup> )	54/109	7.5 (7.2–9.2)	0.64 (0.47–0.87)	0.66 (0.48–0.91)	<i>0.0112</i>

\* Adjusted for IMDC risk group, presence of bone metastases and number of previous VEGFR TKI treatment (1 or 2)



**Table 2.**

Treatment comparison on PFS and OS by MVD and MCD levels (dichotomized at the upper 33% value) by treatment arm.

	CABOZANTINIB (N=175)		EVEROLIMUS (N=185)		CABOZANTINIB vs EVEROLIMUS			
	N of events/N of patients	Months, Median (95% CI)	N of events/N of patients	Months, Median (95% CI)	Hazard ratio- Adjusted* (C vs E) (95%CI)	p- interaction	Hazard ratio- Unadjusted* (C vs E) (95%CI)	p- interaction
<b>Microvascular density</b>								
<b>PFS</b>								
Low (< 208.2 mm <sup>2</sup> )	65/112	7.3 (5.5–7.5)	89/128	3.75 (3.6–4.5)	0.45 (0.32–0.64)	<i>0.4961</i>	0.47 (0.34–0.65)	<i>0.3639</i>
High (>208.2 mm <sup>2</sup> )	32/63	8.97 (6.28–NR)	34/57	7.3 (4.1–9.1)	0.56 (0.34–0.91)		0.62 (0.38–0.99)	
Adj HR (High vs Low)*		0.77 (.50–1.18)		0.63 (0.42–0.95)				
<b>OS</b>								
Low (< 208.2 mm <sup>2</sup> )	49/112	20.8 (17.1–NR)	72/128	16.4 (13.2–18.9)	0.61 (0.42–0.89)	<i>0.7628</i>	0.69 (0.48–0.99)	<i>0.7745</i>
High (>208.2 mm <sup>2</sup> )	21/63	NR (18.2–NR)	27/57	20.4 (13.9–NR)	0.55 (0.31–0.97)		0.62 (0.35–1.10)	
Adj HR (High vs Low)*		0.75 (.45–1.26)		0.84 (0.54–1.31)				
<b>Mast cell Density</b>								
<b>PFS</b>								
Low (< 11.3 mm <sup>2</sup> )	60/102	7.2 (5.6–8.5)	82/114	3.8 (3.6–4.7)	0.43 (0.30–0.60)	<i>0.1127</i>	0.44 (0.32–0.62)	<i>0.1121</i>
High (>11.3 mm <sup>2</sup> )	27/57	7.5 (7.2–NR)	27/52	7.5 (5.6–9.2)	0.71 (0.41–1.22)		0.74 (0.44–1.26)	
Adj. HR (High vs Low)*		0.85 (0.54–1.34)		0.51 (0.32–0.79)				
<b>OS</b>								
Low (< 11.3 mm <sup>2</sup> )	43/102	20.1 (17.4–NR)	67/114	15.4 (11.6–18.8)	0.52 (0.35–0.77)	<i>0.2406</i>	0.59 (0.40–0.87)	<i>0.3691</i>
High (>11.3 mm <sup>2</sup> )	19/57	NR (17.2–NR)	20/52	NR (16.2–NR)	0.82 (0.43–1.54)		0.83 (0.44–1.55)	
Adj. HR (High vs Low)*		0.88 (0.51–1.52)		0.56 (0.34–0.94)				

\* Adjusted for IMDC risk group, presence of bone metastases and number of previous VEGFR TKI treatment (1 or 2)